

ORIGINAL ARTICLE

DLEU7-AS1 promotes renal cell cancer by silencing the miR-26a-5p/coronin-3 axis

Xin-jun Wang^{1,2}, Lin Chen^{2,1}, Ran Xu¹, Si Li¹ and Guang-cheng Luo^{1,2}

¹Department of Urology, Zhongshan Hospital Xiamen University, School of medicine, Xiamen University, Xiamen, Fujian, China and ²The Third Clinical Medical College, Fujian Medical University, Fuzhou, Fujian, China

Correspondence to: Guang-cheng Luo; E-mail: lgch@xmu.edu.cn

ABSTRACT

Long non-coding RNAs (lncRNAs) have been implicated in the progression and development of many types of cancer by interacting with RNA, DNA and proteins, including DLEU7-AS1. However, the function of DLEU7-AS1 in renal cell cancer (RCC) remains unclear. In this study, two *in silico* prediction algorithms were used to discover the potential target of miR-26a-5p, which was determined to be a tumor suppressor gene, possibly DLEU7-AS1, through the downregulation of coronin-3 in RCC. Thus, we hypothesized that DLEU7-AS1 promotes RCC by silencing the miR-26a-5p/coronin-3 axis. To test our hypothesis, we confirmed that DLEU7-AS1 directly targets miR-26a-5p using the pmirGLO dual-luciferase reporter assay. Next, we observed that DLEU7-AS1 expression was markedly upregulated in RCC samples and inversely correlated with clinical prognosis and miR-26a-5p levels. Knockdown of DLEU7-AS1 significantly suppressed the growth and metastasis of RCC cells *in vitro* and attenuated tumor growth *in vivo*. Interestingly, exogenous expression of coronin-3 or miR-26a-5p inhibitor treatment almost completely rescued the DLEU7-AS1 knockdown-induced inhibitory effects on cell proliferation, migration and invasion. In conclusion, our data demonstrate that DLEU7-AS1 is an oncogene in RCC capable of regulating the growth and metastasis of RCC by silencing the miR-26a-5p/coronin-3 axis, suggesting that DLEU7-AS1 can be employed as a potential therapeutic target and prognostic biomarker for RCC.

Keywords: coronin-3, DLEU7-AS1, miR-26a-5p, renal cell cancer

INTRODUCTION

More than 90% of kidney cancers are renal cell cancers (RCCs), which start when malignant cells form in tubules [1]. An assessment by the World Health Organization (WHO) revealed that, in 2020, >430 000 individuals troubled by kidney cancer [2]. Although many treatments have been used for RCC, such as surgery, radiation therapy, immunotherapy and targeted therapy, the 5-year survival rate is not high after diagnosis [3, 4]. Therefore, there is an urgent need to investigate the underlying molecular mechanisms of RCC and to exploit novel drugs or therapeutic methods. MicroRNAs (miRNAs) are small

single-stranded non-coding RNAs with ~18–22 nucleotides that have essential roles in regulating the initiation, progression and metastasis of tumors [5]. Our group demonstrated that miR-26a-5p inhibits RCC by downregulating coronin-3 [6]. However, the expression of miRNAs is regulated by multiple molecular mechanisms [7], which requires a deep understanding of miR-26a-5p regulation. In this study, our data demonstrated that DLEU7-AS1 can directly bind to miR-26a-5p to prevent its interaction with its target and thus plays a role in RCC.

Long non-coding RNAs (lncRNAs) are a category of RNAs with >200 nucleotides that have no protein-coding capacity [8]. Recent studies have identified that many lncRNAs play important

Received: 28.1.2022; Editorial decision: 22.2.2022

© The Author(s) 2022. Published by Oxford University Press on behalf of the ERA. This is an Open Access article distributed under the terms of the Creative Commons Attribution-NonCommercial License (<https://creativecommons.org/licenses/by-nc/4.0/>), which permits non-commercial re-use, distribution, and reproduction in any medium, provided the original work is properly cited. For commercial re-use, please contact journals.permissions@oup.com

roles in human diseases, particularly cancers [9–11]. As a member of the lncRNAs, DLEU7-AS1 was found to be an oncogene in colorectal cancer [12]. However, the function of DLEU7-AS1 in RCC has not been systematically studied. In this study, we demonstrated that DLEU7-AS1 is considerably upregulated in RCC samples compared with normal tissues. *In vitro*, DLEU7-AS1 knockdown inhibited cell growth and metastasis but promoted apoptosis. *In vivo*, DLEU7-AS1 downregulation attenuated tumor growth. Thus, our findings suggest that DLEU7-AS1 may be a key determinant of RCC progression, providing lncRNA-based therapeutic approaches that target the DLEU7-AS1/miR-26a-5p/coronin-3 pathway.

MATERIALS AND METHODS

TCGA database analysis

RCC tumor and normal samples [containing clinical and messenger RNA (mRNA) expression information] were obtained from the mRNA-seq data from the TCGA-KIRC database (<https://portal.gdc.cancer.gov/>). The database contains 72 normal and 539 RCC samples. TCGA-clinical data (<https://tcga.xenahubs.net>) were extracted for overall survival (OS) analysis.

Patient samples

RCC tissues (28) and normal tissues (27) were collected from the Department of Urology, Zhongshan Hospital, Xiamen University (Xiamen, China) and stored as described previously [13]. Informed consent was obtained from patients, and the study was approved by the Institutional Review Board of Xiamen University.

Cell culture and generation of stable cells

The 786-O, HEK293T and Caki-1 cell lines were acquired from ATCC (<https://www.atcc.org/>). All cells used in this study were cultured in Dulbecco's modified Eagle's medium (DMEM) supplemented with 10% fetal bovine serum at 37°C in a 5% CO₂ atmosphere with 21% O₂. To generate a stable knockdown of DLEU7-AS1 in the 786-O and Caki-1 cell lines, the shDLEU7-AS1 or control plasmid was cloned into the pCDH-EF1-MCS-T2A-Puro expression vector. Briefly, HEK293T cells were co-transfected with 12 μg of DLEU7-AS1 or control plasmid, 8 μg of psPAX2 (Antihela) and 4 μg of pMD2.G using Lipofectamine 3000 (Invitrogen) to generate lentiviruses. The viral supernatants were collected 48 h after transfection and used to infect 786-O and Caki-1 cells using 10 μg/mL polybrene (Yeasen, Shanghai, China). The primers used to generate shDLEU7-AS1 are listed in Supplementary data, Table S1.

Quantitative real-time RT-PCR

The quantitative real-time reverse transcription PCR (real-time qRT-PCR) array was performed as described previously [6]. Trizol was used to isolate total RNA from RCC tissues and cells. Superscript III transcriptase (Invitrogen) was used to synthesize complementary DNA (cDNA), and SYBR Green was used to perform real-time qRT-PCR. Relative quantification was normalized to GAPDH, U6 or 18s rRNA level. The primer sequences used for qRT-PCR are listed in Supplementary data, Table S2.

RNA fluorescence in situ hybridization (RNA-FISH)

RNA-FISH is a tool used for studying the distribution and function of lncRNA [14]. The distribution of DLEU7-AS1 in 786-O and Caki-1 cells was measured using an RNA-FISH kit (Cat#: C10910, Ribobio, Guangzhou, Guangdong, China) following the manufacturer's instructions. U6 and 18s were used as reference genes to distinguish between the nucleus and cytoplasm. The RNA-FISH images were captured using a laser scanning confocal microscope (Leica).

pmirGLO dual-luciferase assay

The 786-O and Caki-1 cell lines were co-transfected with miR-26a-5p-luciferase and either DLEU7-AS1 or DLEU7-AS1-MUT plasmids, and harvested 2 days after transfection for luciferase reporter assays. The relative luciferase activity was determined using the Dual-Glo Luciferase Assay System (Promega). The activity of Renilla luciferase as a control reporter was used for luciferase activity standardization.

Cell viability, cell cycle and apoptosis analysis

The 786-O or Caki-1 cells (1 × 10⁶/well) with shNC or shDLEU7-AS1 were seeded in 96-well plates. miR-26a-5p inhibitor, coronin-3 expression plasmid or their control (4 μg) was transfected using Exfect Transfection Reagent (Vazyme, Nanjing, Jiangsu, China). After 48 h of transfection, the CCK8 array (Yeasen, Shanghai, China) was used to detect cell viability following the manufacturer's instructions. A SpectraMax absorbance reader (Molecular Devices, San Francisco, CA, USA) was used to measure absorbance at 450 nm. The cell cycle and apoptosis were measured using the NovoCyte flow cytometer (Cat#: 1300, ACEA, San Diego, CA, USA) with the Annexin V-FITC/PI apoptosis detection kit (Cat#: A211-02, Vazyme, Nanjing, China). The flow cytometry data were analyzed using NovoExpress 1.4.1 (ACEA).

Cell migration and invasion assays

Transwells (Cat#: 3422, Corning, NY, USA) with 8-μm-pore polycarbonate membranes were used to determine cell migration (without Matrigel) and invasion assays (with Matrigel). Matrigel (Cat#: 356 234) was purchased from BD Biosciences (San Jose, CA, USA). Caki-1 or 786-O cells were cultured in the upper chambers of the transwell with DMEM without serum. Complete DMEM was placed in the lower chambers. Cells that migrated or invaded were counted and photographed after 24 h of incubation.

Subcutaneous tumor formation experiment

BALB/c nude mice (6–8 weeks, male) were obtained from Beijing Vital River Laboratory Animal Technology Co., Ltd and used in the experiments following a protocol approved by the Animal Care and Use Committee of Xiamen University. A total of 4 × 10⁶ 786-O cells were injected subcutaneously into the lower back area of nude mice (n = 6 per group) to perform orthotopic assays. All mice were sacrificed 34 days after injection, and the tumor weight and volume were quantified. All animal experiments were conducted in accordance with the national guidelines for the humane treatment of animals and were approved by the Institutional Review Board of Xiamen University.

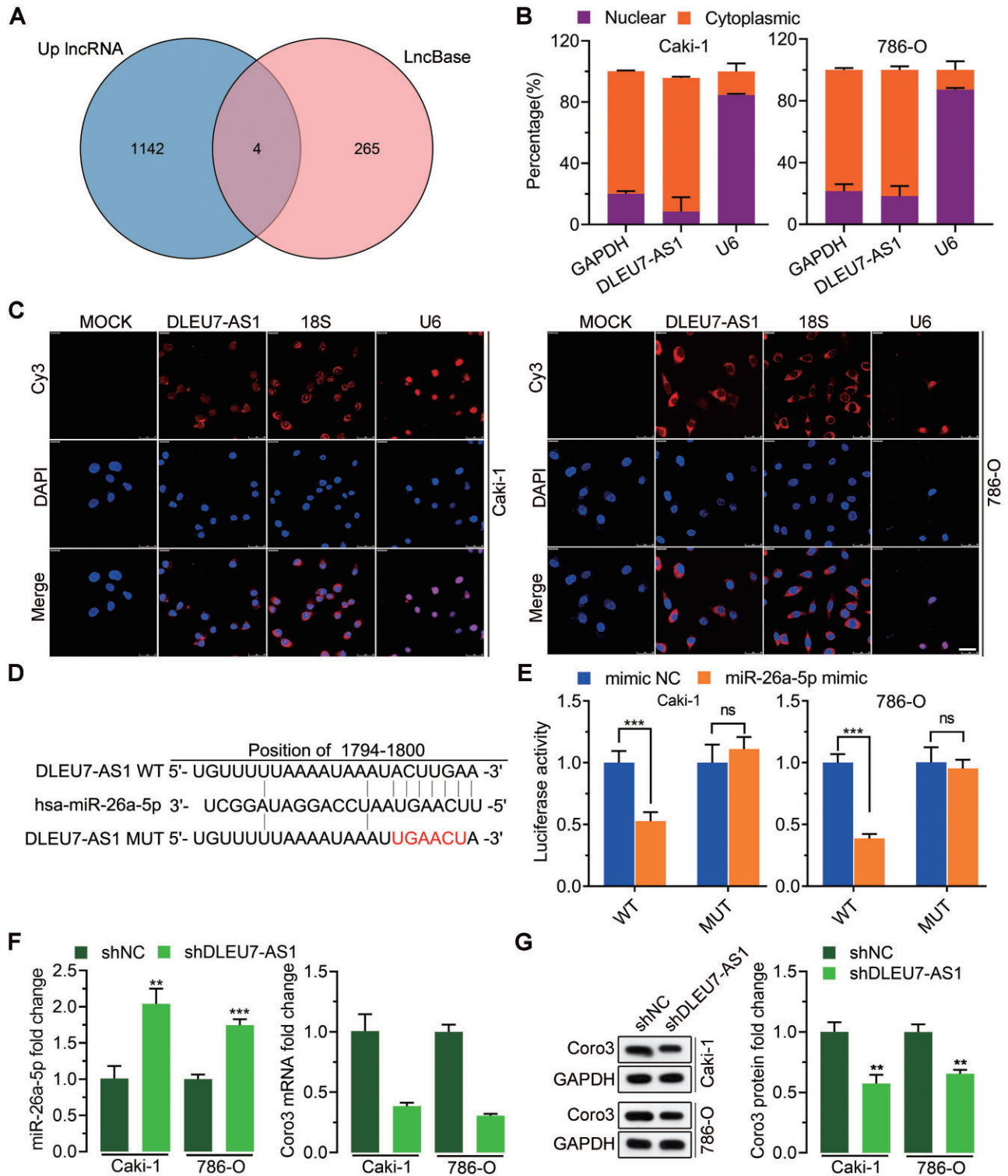


FIGURE 1: DLEU7-AS1 acts as a sponge for miR-26a-5p in RCC. (A) Venn diagram shows long non-coding RNA (lncRNA) targeting miR-26a-5p using lncRNA and LncBase. (B) The location of DLEU7-AS1 was confirmed in Caki-1 and 786-O cells using a subcellular fractionation assay. (C) RNA fluorescence in situ hybridization (FISH) assay confirmed the location of DLEU7-AS1. DLEU7-AS1 was largely located in the cytoplasm of Caki-1 and 786-O cells. Nuclei were stained with DAPI; DLEU7-AS1 was stained red. Reference genes 18S and U6 were stained red. Scale bar represents 25 μ m. (D) The location of the miR-26a-5p target sites in DLEU7-AS1 and the mutation site of DLEU7-AS1. (E) Dual-luciferase reporter assay analyzed the effect of miR-26a-5p ectopic expression on the activity of DLEU7-AS1 WT and MUT in Caki-1 and 786-O cells. (F) The relative levels of miR-26a-5p in Caki-1 and 786-O cells, which were transfected using the negative control (shNC) and shDLEU7-AS1, were identified using real-time qRT-PCR (quantitative reverse transcription polymerase chain reaction). (G) Western blot was used to measure the protein levels of coronin-3 in Caki-1 and 786-O cells that were transfected with shNC and shDLEU7-AS1. Data represent mean \pm SD of three biological replicates. Student's t-test was applied to obtain the P-value: ns: no significant difference, ***P < 0.01, ****P < 0.001.

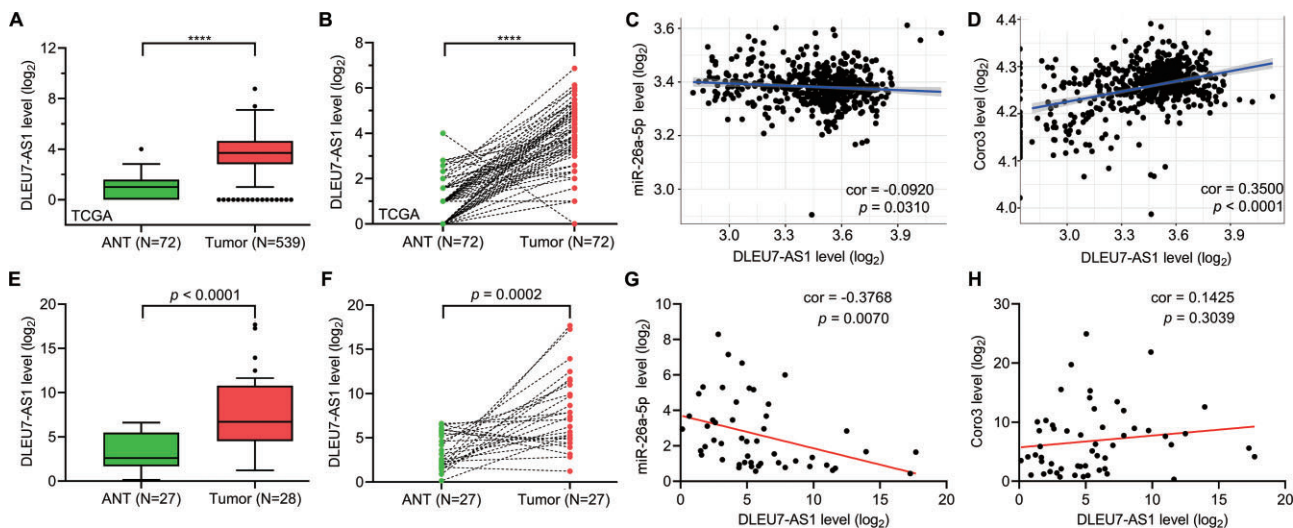


FIGURE 2: The expression level of DLEU7-AS1 in RCC. (A and B) The transcription level of DLEU7-AS1 in unpaired (A) and paired (B) tumor-normal RCC tissues was determined using data obtained from the Cancer Genome Atlas (TCGA) database. Data represent mean \pm SD. (C and D) The correlation between the DLEU7-AS1 level and the expression of miR-26a-5p and coronin-3 was determined using the data obtained from the TCGA database. (E and F) Real-time quantitative reverse transcription polymerase chain reaction (qRT-PCR) analysis of DLEU7-AS1 expression in unpaired tumor-normal/paired tumor-normal RCC tissues. Data represent mean \pm SD of three technical replicates. (G and H) Correlation between DLEU7-AS1 level and the levels of miR-26a-5p and coronin-3 (Coro3). Mann-Whitney test (A and E), Wilcoxon matched-pairs signed-rank test (B and F), **** $P < 0.0001$. Pearson correlation test (C, D, G and H).

Western blotting

Western blotting was performed as described previously [6]. Coronin-3 (Cat:14749-1-AP, Proteintech) and GAPDH (Cat#: YM3029, Immunoway) were used as primary antibodies, the HRP-labeled secondary antibodies were used to detect the chemiluminescence signals.

Immunohistochemical (IHC) staining

Tissue sections were collected from mouse xenograft tumors and fixed with 10% formaldehyde. The tissues were cut into 10 μ m sections and heated at 95°C for 20 min with 10 mM sodium citrate (pH 6.0). Sections were immunostained with anti-coronin-3 (1:200; Cat#:14749-1-AP, Proteintech). Immunostaining was carried out using an ABC peroxidase standard staining kit in accordance with the manufacturer's instructions.

Statistical analysis

SPSS software b22.0 (IBM SPSS, Armonk, NY, USA) was used for statistical analysis. Graphs were drawn using GraphPad Prism 5 (GraphPad Software, Inc., La Jolla, CA, USA). Measurements are expressed as mean \pm standard deviation (SD). Student's *t*-test, Mann-Whitney test, Wilcoxon matched-pairs signed-rank test and Kruskal-Wallis one-way ANOVA followed by Dunn's multiple comparison test were used to identify the *P*-value, and statistical significance was set at $P < 0.05$.

RESULTS

DLEU7-AS1 functions as a sponge for miR-26a-5p

Our previous data demonstrated that miR-26a-5p inhibits RCC by downregulating coronin-3 [6]. However, the lncRNA on the lncRNA-miR-26a-5p-coronin-3 axis as a master regulator of RCC is still unknown. To identify lncRNAs acting on the miR-26a-5p/Cro3 axis, two *in silico* algorithms (UplncRNA and LncBase)

were used to predict the lncRNAs that interact with miR-26a-5p. Two *in silico* prediction algorithms identified four lncRNAs (miTG-score ≥ 0.85) that contain putative binding sites for miR-26a-5p, including DLEU7-AS1, LINC00971, DOCK4-AS1 and VSTM2A-OT1 (Figure 1A). Importantly, the nuclear and cytoplasmic separation experiments (Figure 1B) and FISH (Figure 1C) in 786-O and Caki-1 cells showed that DLEU7-AS1 is mainly distributed in the cytoplasm, indicating that it may act as a competitive endogenous RNA and a regulator of miR-26a-5p. Thus, DLEU7-AS1 was chosen for further investigation. Then, the luciferase reporter plasmid containing the wild type (WT) of DLEU7-AS1 or the mutated (MUT) miR-26a-5p binding site at position-1794-1800 (DLEU7-AS1_MUT) was constructed (Figure 1D). Dual-luciferase reporter assays demonstrated that miR-26a-5p overexpression remarkably decreased the luciferase activity of DLEU7-AS1-WT in 786-O and Caki-1 cells, but not the activity of DLEU7-AS1-MUT (Figure 1E). Subsequently, we assessed the level of miR-26a-5p in both 786-O and Caki-1 cells, which were transfected with the negative control (shNC) or shDLEU7-AS1, using qRT-PCR. Our data demonstrated that miR-26a-5p is regulated by DLEU7-AS1 (Figure 1F). Western blot analysis revealed that DLEU7-AS1 can regulate the protein levels of coronin-3, which has been identified as a direct target of miR-26a-5p (Figure 1G). Therefore, our results demonstrate that DLEU7-AS1 functions as a sponge for miR-26a-5p in RCC.

DLEU7-AS1 is upregulated in RCC

To study the differences in DLEU7-AS1 expression, a total of 539 tumors and 72 normal samples were acquired from TCGA-KIRC. As shown in Figure 2A, we found that DLEU7-AS1 mRNA was significantly upregulated in RCC tumor samples compared with normal tissues. DLEU7-AS1 expression in 72 pairs of RCC samples was analyzed, and it was found that DLEU7-AS1 was significantly upregulated in RCC tumor samples (Figure 2B). We subsequently investigated the correlation between the DLEU7-AS1 level and miR-26a-5p and coronin-3 levels. Our results

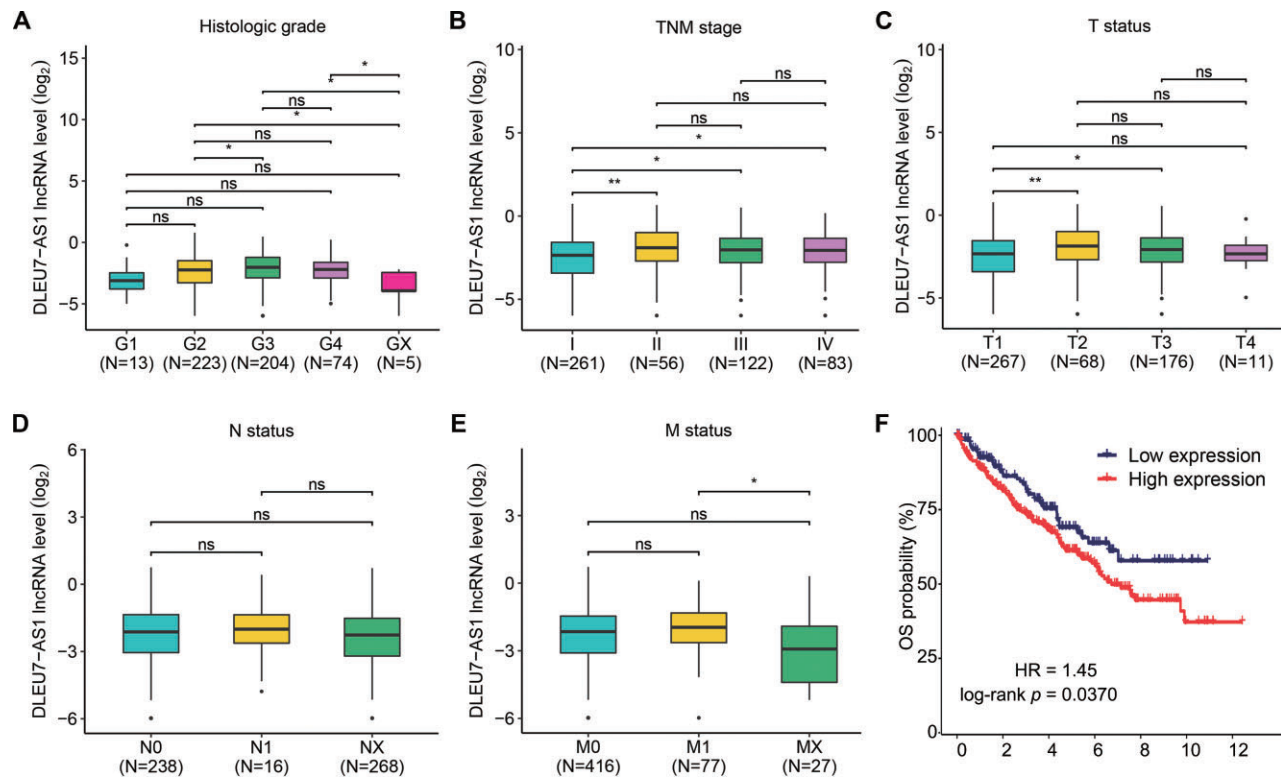


FIGURE 3: Association between the level of DLEU7-AS1 and the clinicopathological characteristics of patients afflicted with RCC. Overview of DLEU7-AS1 expression (TCGA database) according to histologic grade (A), TNM stage (B), T status (C), N status (D) and M status (E). Data represent mean \pm SD. Kruskal–Wallis one-way ANOVA followed by Dunn’s multiple comparison test: ns, no significant difference; * $P < 0.05$, ** $P < 0.01$. (F) Kaplan–Meier analysis of the OS of patients afflicted with RCC from the TCGA database by high or low expression of DLEU7-AS1. Log-rank test.

showed that the expression of DLEU7-AS1 was inversely correlated with the expression of miR-26a-5p (Figure 2C) and positively correlated with the expression of coronin-3 (Figure 2D). To verify our results, we detected DLEU7-AS1 expression using qRT-PCR in 27 paired RCC tissues and matching normal tissues. As shown in Figure 2E and F, the levels of DLEU7-AS1 are up-regulated in RCC tissues compared with normal tissues. Interestingly, the correlation analysis revealed an inverse correlation between the levels of DLEU7-AS1 and miR-26a-5p (Figure 2G). However, due to the limited number of RCC cases, no strong correlation was observed between DLEU7-AS1 and coronin-3 (Figure 1H). Altogether, these data demonstrate that DLEU7-AS1 was up-regulated in RCC, and the expression of DLEU7-AS1 was negatively correlated with the level of miR-26a-5p and was positively correlated with the level of coronin-3.

The association of DLEU7-AS1 level with clinicopathological characteristics

DLEU7-AS1 has been observed to be upregulated in RCC tissues, but the association of DLEU7-AS1 level with clinicopathological characteristics remains unknown. Next, a total of 522 RCC tissues with both clinical and gene expression data were used to analyze the association of DLEU7-AS1 levels with clinicopathological characteristics. As shown in Figure 3A–E, increased DLEU7-AS1 expression significantly correlated with the histologic grade, TNM stage, T status and M status, but no significant correlation was observed in N status. Meanwhile, Kaplan–Meier survival analysis showed that RCCs with high DLEU7-AS1 ex-

pression had a poorer OS than those with low DLEU7-AS1 expression (hazard ratio: 1.45, $P = 0.037$) (Figure 3F). The correlation between clinicopathological variables and DLEU7-AS1 expression was summarized in Table 1. These results indicate that RCCs with high DLEU7-AS1 expression more easily develop to an advanced stage and distant metastasis than RCCs with low DLEU7-AS1 expression.

DLEU7-AS1 serves as an oncogene in RCC via miR-26a-5p/coronin-3 axis in vitro

Loss-of-function experiments were performed to examine the function of DLEU7-AS1 in RCC cells *in vitro* and *in vivo*. For this objective, the lentivirus-based antagomir expression system was used to stably knock down DLEU7-AS1 in Caki-1 and 786-O cells. As can be seen in Supplementary data, Figure S1A, DLEU7-AS1 expression was reduced by DLEU7-AS1 shRNA (shDLEU7-AS1-1, shDLEU7-AS1-2 and shDLEU7-AS1-3) compared with negative control shRNA (shNC). shDLEU7-AS1-2 was chosen for further work because of its highest knockdown efficiency. Moreover, the effects of shDLEU7-AS1 were partly disrupted by the addition of the miR-26a-5p inhibitor. DLEU7-AS1 knockdown increased miR-26a-5p expression and reduced the expression of coronin-3, and when the miR-26a-5p inhibitor was added, the expression of coronin-3 notably increased (Supplementary data, Figure S1B). In addition, coronin-3 overexpression also rescued the reduction of coronin-3 mRNA (Supplementary data, Figure S1B). Next, cell viability in each group was evaluated using the CCK8 assay. The results showed that knockdown of DLEU7-AS1 led to

Table 1. Correlation between clinicopathological variables and DLEU7-AS1 expression in RCC

	Total (N = 522)	DLEU7-AS1 expression		P-value ^a
		High (N = 363)	Low (N = 159)	
Age (years)				0.0371
<65	328 (62.8%)	217 (59.8%)	111 (69.8%)	
≥65	194 (37.2%)	146 (40.2%)	48 (30.2%)	
Gender				1.0000
Male	340 (65.1%)	236 (65.0%)	104 (65.4%)	
Female	182 (34.9%)	127 (35.0%)	55 (34.6%)	
TNM stage				0.0032
I	261 (50.0%)	162 (44.6%)	99 (62.3%)	
II	56 (10.7%)	43 (11.8%)	13 (8.2%)	
III	122 (23.4%)	94 (25.9%)	28 (17.6%)	
IV	83 (15.9%)	64 (17.6%)	19 (11.9%)	
Histologic grade				0.0053
G1-G2	236 (45.2%)	152 (41.9%)	84 (52.8%)	
G3-G4	278 (53.3%)	208 (57.3%)	70 (44.0%)	
Unknown	8 (1.5%)	3 (0.8%)	5 (3.1%)	
Pathologic T				0.0052
T1	267 (51.1%)	167 (46.0%)	100 (62.9%)	
T2	68 (13.0%)	53 (14.6%)	15 (9.4%)	
T3	176 (33.7%)	135 (37.2%)	41 (25.8%)	
T4	11 (2.1%)	8 (2.2%)	3 (1.9%)	
Pathologic N				0.2740
N0	238 (45.6%)	171 (47.1%)	67 (42.1%)	
N1	16 (3.1%)	13 (3.6%)	3 (1.9%)	
NX	268 (51.3%)	179 (49.3%)	89 (56.0%)	
Pathologic M				0.0020
M0	416 (79.7%)	288 (79.3%)	128 (80.5%)	
M1	77 (14.8%)	62 (17.1%)	15 (9.4%)	
MX	27 (5.2%)	13 (3.6%)	14 (8.8%)	
Unknown	2 (0.4%)	0 (0%)	2 (1.3%)	
Living status				0.0276
Alive	350 (67.0%)	232 (63.9%)	118 (74.2%)	
Dead	172 (33.0%)	131 (36.1%)	41 (25.8%)	
Disease status				0.477
No	96 (18.4%)	62 (17.1%)	34 (21.4%)	
Yes	15 (2.9%)	10 (2.8%)	5 (3.1%)	
Unknown	411 (78.7%)	291 (80.2%)	120 (75.5%)	
DSS				0.1850
No	404 (77.4%)	276 (76.0%)	128 (80.5%)	
Yes	107 (20.5%)	81 (22.3%)	26 (16.4%)	
Unknown	11 (2.1%)	6 (1.7%)	5 (3.1%)	
PFI				0.1140
No	364 (69.7%)	245 (67.5%)	119 (74.8%)	
Yes	158 (30.3%)	118 (32.5%)	40 (25.2%)	

^aChi-squared test. Statistically significant P-values are given in bold italic. DSS, disease-specific survival. PFI, progression-free interval.

a significant decrease in cell proliferation in both Caki-1 and 786-O cells, and the proliferation inhibitory effects of DLEU7-AS1 knockdown were rescued using the miR-26a-5p inhibitor and ectopic expression of coronin-3 (Figure 4A). Furthermore, the effects of DLEU7-AS1 knockdown on cell cycle progression were assessed using flow cytometry. As Figure 4B shows, our data reveals that knockdown of DLEU7-AS1 repressed cell G1/S phase transition in both 786-O and Caki-1 cells, and that the miR-26a-5p inhibitor or exogenous expression of coronin-3 rescued the DLEU7-AS1 knockdown-induced inhibitory effects on the cell cycle of both Caki-1 and 786-O cells. Furthermore, flow cytometry data revealed that DLEU7-AS1 knockdown caused a significant

increase in cell apoptosis in both Caki-1 and 786-O cells (Figure 4C). Interestingly, transfection of miR-26a-5p inhibitor or exogenous expression of coronin-3 almost completely rescued the DLEU7-AS1 knockdown-induced effects on cell apoptosis (Figure 4C). These data demonstrate that knockdown of DLEU7-AS1 inhibited the growth and promoted apoptosis of RCC cells through the miR-26a-5p/coronin-3 axis *in vitro*.

Next, it was studied whether DLEU7-AS1 knockdown could inhibit the invasiveness of RCC cell lines by regulating the miR-26a-5p/coronin-3 axis. Transwell assays showed that DLEU7-AS1 knockdown in 786-O and Caki-1 cells markedly suppressed cell migration (Figure 5A) and invasion (Figure 5B). Rescue experiments were performed using the miR-26a-5p inhibitor and coronin-3 expression plasmid to confirm that knockdown of DLEU7-AS1 suppresses the metastasis of RCC cells by directly targeting the miR-26a-5p/coronin-3 axis. Interestingly, the miR-26a-5p inhibitor or exogenous expression of Coro3 partially rescued the DLEU7-AS1 knockdown-induced inhibitory effects on the migration and invasion of Caki-1 and 786-O cells *in vitro* (Figure 5A and B). Therefore, our data demonstrates that the miR-26a-5p/coronin-3 axis is a functional target of DLEU7-AS1.

Knockdown of DLEU7-AS1 inhibits the tumor growth of RCC *in vivo*

To evaluate whether shDLEU7-AS1 could suppress tumor growth of RCC cells *in vivo*, 786-O cells with stable DLEU7-AS1 knockdown (shDLEU7-AS1) or negative control (shNC) cells were injected into nude mice. The mice were sacrificed after 34 days. The images of isolated tumors showed that knockdown of DLEU7-AS1 inhibited tumor growth (Figure 6A). The tumor volume (Figure 6B) and tumor weight (Figure 6C) were inhibited in the DLEU7-AS1 knockdown group compared with the control group. Furthermore, the expression of DLEU7-AS1, miR-26a-5p and coronin-3 was detected using qRT-PCR in xenograft tumors. Our results revealed that shDLEU7-AS1 significantly reduced the level of DLEU7-AS1, enhanced the level of miR-26a-5p and decreased the mRNA level of coronin-3 in xenograft tumors (Figure 6D-F). The protein expression of coronin-3 was examined in xenograft tumors using western blotting. Figure 6G and H shows that the protein level of coronin-3 was significantly reduced in xenograft tumors injected with 786-O-DLEU7-AS1 knockdown cells compared with 786-O shNC cells. Ki-67-positive tumor cells were analyzed and quantified using IHC staining in xenograft tumors, and our results showed that proliferation-related Ki-67 was inhibited upon DLEU7-AS1 knockdown (Figure 6I and J). These data from *in vivo* experiments reveal that knockdown of DLEU7-AS1 significantly inhibits the tumor growth of RCC cells by regulating the miR-26-5p/coronin-3 pathway.

DISCUSSION

We identified a DLEU7-AS1/miR-26a-5p/coronin-3 axis in RCC. miR-26a-5p regulates the growth and metastasis of RCC by directly binding to the 3'-untranslated region of coronin-3 mRNA to act as a tumor suppressor gene in RCC [6]. It has been reported that miRNAs are very important for the initiation and progression of tumors, including breast cancer and non-small cell lung cancer [5, 15, 16]. Thus, inappropriate control of miRNAs may cause cancer [17]. miRNA expression is regulated by multiple factors, including lncRNAs. Therefore, it is important to study the upstream regulatory factors of miRNAs. In this study, it was found that DLEU7-AS1, LINC0097, 1DOCK4-AS1 and

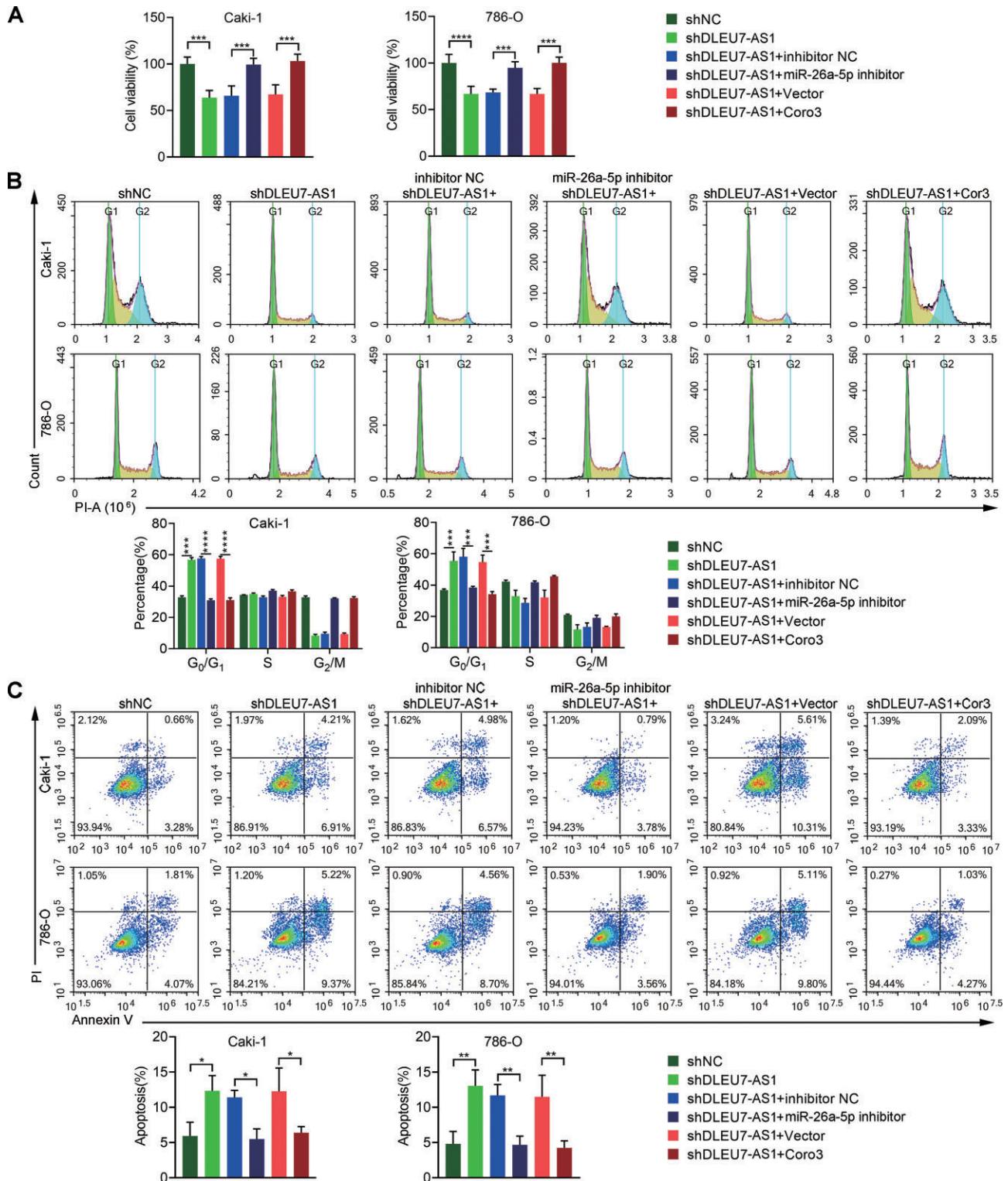


FIGURE 4: DLEU7-AS1 knockdown suppresses proliferation and promotes apoptosis in RCC cells via the miR-26a-5p/Coro3 axis. (A) DLEU7-AS1 deficiency inhibits cell viability via the miR-26a-5p/Coro3 axis. Data represent mean \pm SD of four biological replicates. (B) DLEU7-AS1 knockdown induces cell-cycle arrest at the G₀/G₁ phase via the miR-26a-5p/Coro3 axis. Data represent mean \pm SD of three biological replicates. (C) DLEU7-AS1 knockdown increases cell apoptosis via the miR-26a-5p/Coro3 axis. Data represent mean \pm SD of three biological replicates. One-way ANOVA followed by Tukey's post-hoc test was applied for P-value: *P < 0.05, **P < 0.01, ***P < 0.001, ****P < 0.0001.

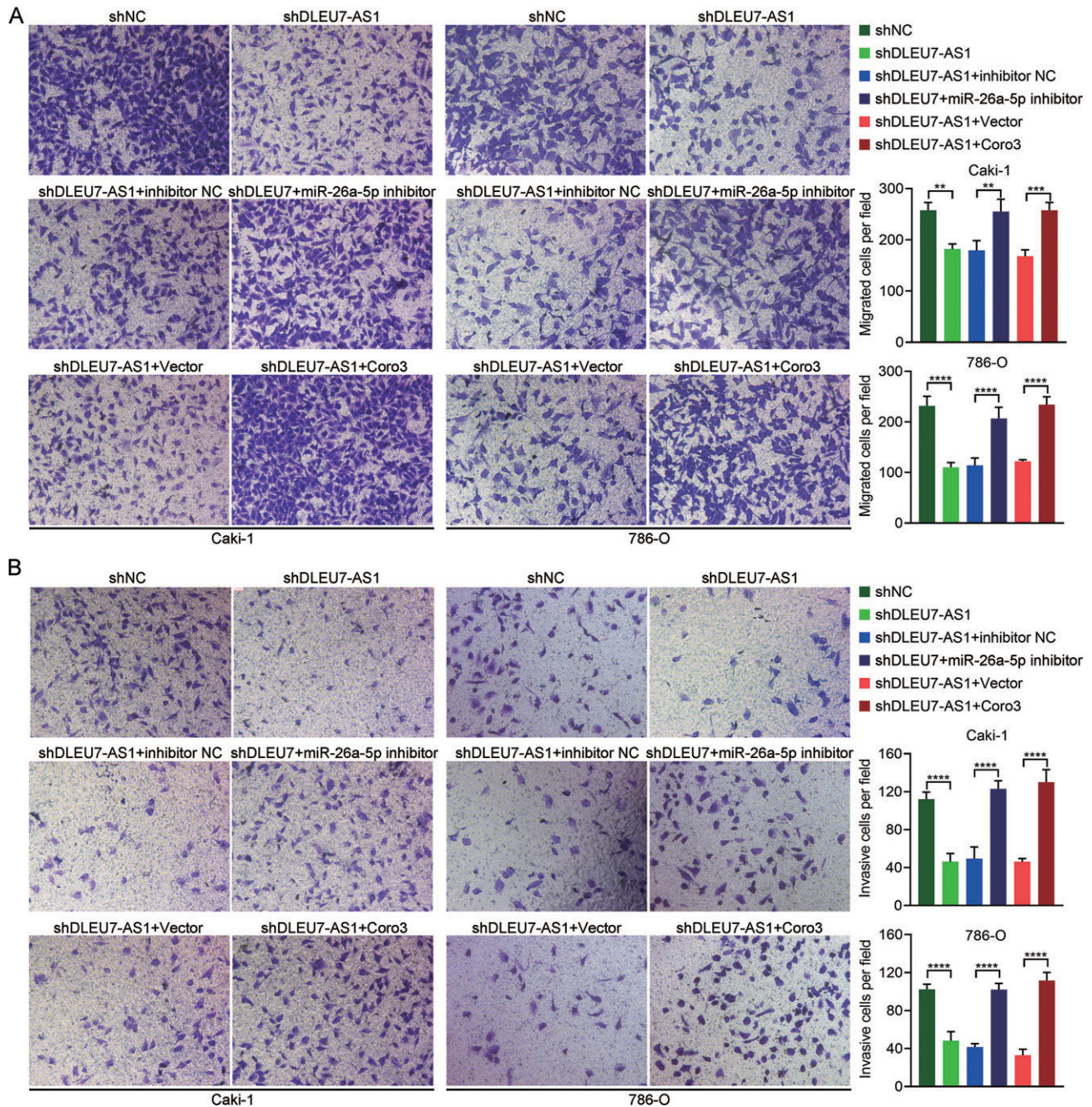


FIGURE 5: DLEU7-AS1 knockdown suppresses the ability of cell migration and invasion in RCC via the miR-26a-5p/Coro3 axis. (A) Transwell migration assays revealed that DLEU7-AS1 knockdown inhibits the migration ability of Caki-1 and 786-O cells. The effect of DLEU7-AS1 knockdown on the migration ability of Caki-1 and 786-O cell lines was rescued by using miR-26a-5p inhibitor and coronin-3. (B) Transwell Invasion assays demonstrated that DLEU7-AS1 knockdown inhibits the invasion of 786-O and Caki-1 cells. The effect of DLEU7-AS1 knockdown on the invasion ability of Caki-1 and 786-O cells was rescued by miR-26a-5p inhibitor and coronin-3. Data represent mean \pm SD of three biological replicates, one-way ANOVA followed by Tukey's post-hoc test: ** $P < 0.01$, *** $P < 0.001$, **** $P < 0.0001$.

VSTM2A-OT1 have highly conserved miR-26a-5p binding sites using UplncRNA and the LncBase database. Dual-luciferase reporter assays were used to identify DLEU7-AS1 directly targeting miR-26a-5p. These results support the hypothesis that DLEU7-AS1 functions as an oncogene in RCC by regulating the miR-26a-5p/coronin-3 axis (Figure 7).

Many reports have confirmed that lncRNAs as tumor suppressors or oncogenes play important roles in many tumors by interacting with RNA, DNA and proteins [18–20]. In this study, compared with normal tissues, DLEU7-AS1 was remarkably up-regulated in RCC tissues and negatively correlated with OS. Importantly, DLEU7-AS1 knockdown inhibited the proliferation and

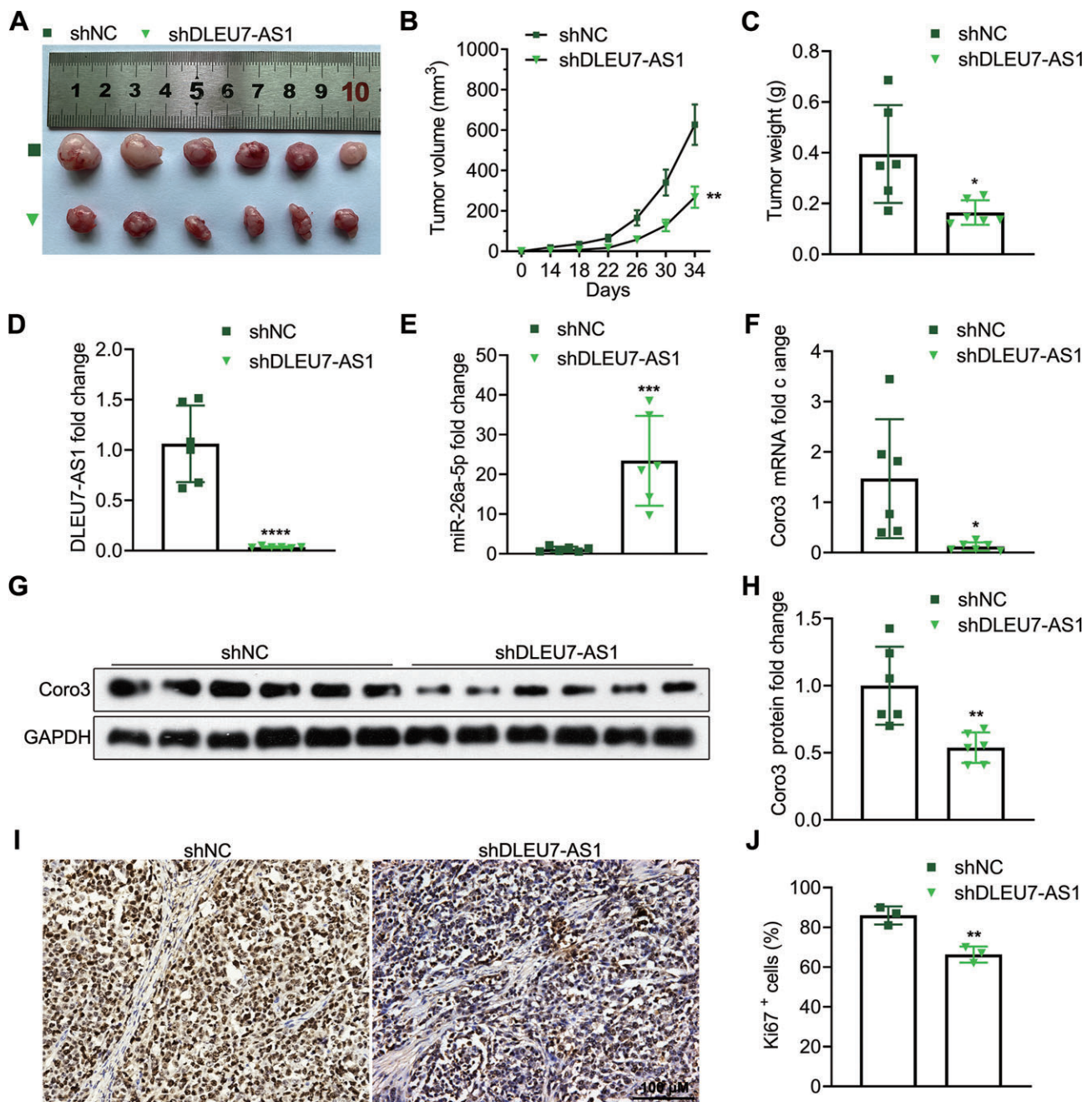


FIGURE 6: DLEU7-AS1 knockdown inhibits the tumor growth of RCC in vivo. (A) Images of isolated tumors. (B and C) Quantitation of tumor volumes (B) every 4 days and tumor weights (C) 34 days after injection with stably DLEU7-AS1 knockdown 786-O cells or negative control cells. Data represent mean \pm SD of six mice. (D and F) Determining of DLEU7-AS1, miR-26a-5p and Coro3 mRNA expression in tumors using RT-qPCR. Data represent mean \pm standard error of mean of six mice. (G and H) Coro3 protein levels were detected using western blotting. Data represent mean \pm SD of six mice. (I and J) Ki67-positive tumor cells were analyzed and quantified using IHC staining. Data represent mean \pm SD of three mice. Student's t-test: * $P < 0.05$, ** $P < 0.01$, *** $P < 0.001$, **** $P < 0.0001$.

metastasis of RCC cells and facilitated their apoptosis by targeting the miR-26a-5p/coronin-3 axis. Furthermore, DLEU7-AS1 knockdown suppressed RCC growth in vivo. In conclusion, our study demonstrated that DLEU7-AS1 is an oncogene in RCC. As an oncogene, DLEU7-AS1 can directly target miR-26a-5p and

inhibit the growth and metastasis of RCC in vivo and in vitro by regulating the miR-26a-5p/coronin-3 axis. Therefore, our data suggest that DLEU7-AS1 may act as a potential diagnostic and therapeutic target and prognostic marker for RCC, paving the way for new therapeutic approaches for RCC.

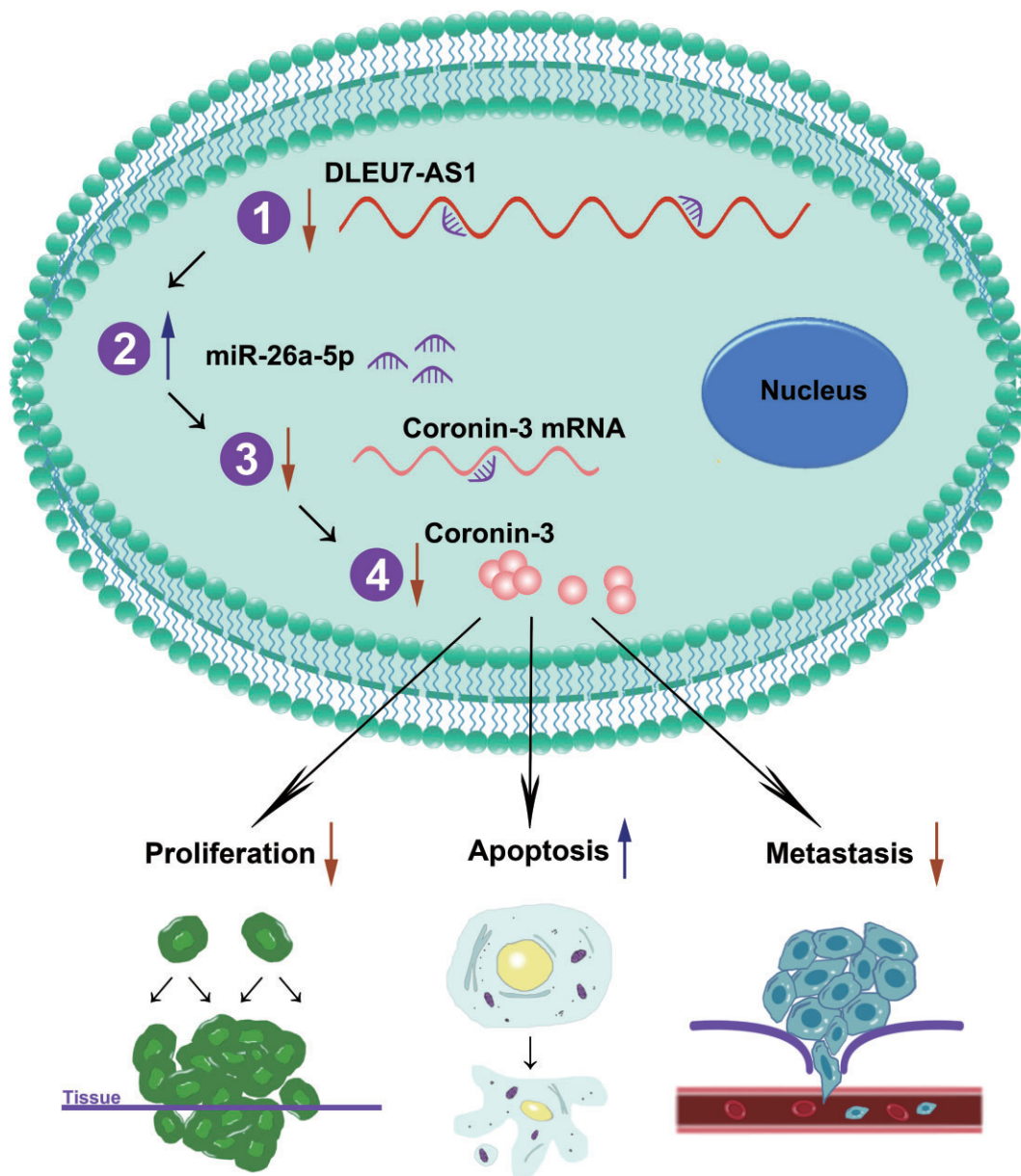


FIGURE 7: Diagrammatic sketch of the regulation of DLEU7-AS1 on miR-26-5p/Coro3 axis.

SUPPLEMENTARY DATA

Supplementary data are available at [ckj](#) online.

ACKNOWLEDGEMENTS

This work was supported by Project of Science and Technology Bureau of Xiamen (3502Z20184033 and 3502Z20194022), the Natural Science Foundation of Fujian Province (2020J011213) and the Young/Middle-aged Talent Cultivation Project funded by Fujian Provincial Health and Family Planning Commission and Xiamen Health and Family Planning Commission (2021GGB028).

AUTHORS' CONTRIBUTIONS

G.-c.L. conceived and designed the study. G.-c.L. and X.-j.W. analyzed the data and wrote the manuscript. X.-j.W., R.X. and S.L.

performed the experiments and collected the data. All authors read and approved the final manuscript.

CONFLICT OF INTEREST STATEMENT

The authors declare that there is no conflict of interest.

DATA AVAILABILITY STATEMENT

The data that support the findings of this study are available from the corresponding author upon reasonable request.

REFERENCES

- Hsieh JJ, Purdue MP, Signoretti S et al. Renal cell carcinoma. *Nat Rev Dis Primers* 2017; 3: 17009

2. Sung H, Ferlay J et al. Global Cancer Statistics 2020: GLOBOCAN Estimates of Incidence and Mortality Worldwide for 36 Cancers in 185 Countries. *CA: A Cancer Journal for Clinicians* 2021; **71**(3): 209–249
3. Padala SA, Barsouk A, Thandra KC et al. Epidemiology of renal cell carcinoma. *World J Oncol* 2020; **11**: 79–87
4. Barata PC, Rini BI. Treatment of renal cell carcinoma: current status and future directions. *CA Cancer J Clin* 2017; **67**: 507–524
5. Peng Y, Croce CM. The role of microRNAs in human cancer. *Signal Transd Target Ther* 2016; **1**: 15004
6. Wang XJ, Yan ZJ, Luo GC et al. miR-26 suppresses renal cell cancer via down-regulating coronin-3. *Mol Cell Biochem* 2020; **463**: 137–146
7. Gulyaeva LF, Kushlinskiy NE. Regulatory mechanisms of microRNA expression. *J Transl Med* 2016; **14**: 143
8. Ponting CP, Oliver PL, Reik W. Evolution and functions of long noncoding RNAs. *Cell* 2009; **136**: 629–641
9. Gutschner T, Diederichs S. The hallmarks of cancer: a long non-coding RNA point of view. *RNA Biol* 2012; **9**: 703–719
10. Schmitt AM, Chang HY. Long noncoding RNAs in cancer pathways. *Cancer Cell* 2016; **29**: 452–463
11. Wapinski O, Chang HY. Long noncoding RNAs and human disease. *Trends Cell Biol* 2011; **21**: 354–361
12. Liu XB, Han C, Sun CZ. Long non-coding RNA DLEU7-AS1 promotes the occurrence and development of colorectal cancer via Wnt/beta-catenin pathway. *Eur Rev Med Pharmacol Sci* 2018; **22**: 110–117
13. Wang X, Xiao Y, Li S et al. CORO6 promotes cell growth and invasion of clear cell renal cell carcinoma via activation of WNT signaling. *Front Cell Dev Biol* 2021; **9**: 647301
14. Tripathi V, Fei J, Ha T et al. RNA fluorescence in situ hybridization in cultured mammalian cells. *Methods Mol Biol* 2015; **1206**: 123–136
15. Ye MF, Lin D, Li WJ et al. MiR-26a-5p serves as an oncogenic microRNA in non-small cell lung cancer by targeting FAF1. *Cancer Manag Res* 2020; **12**: 7131–7142
16. Zhang C, Zhang Y, Ding W et al. MiR-33a suppresses breast cancer cell proliferation and metastasis by targeting ADAM9 and ROS1. *Protein Cell* 2015; **6**: 881–889
17. Croce CM. Causes and consequences of microRNA dysregulation in cancer. *Nat Rev Genet* 2009; **10**: 704–714
18. Huarte M. The emerging role of lncRNAs in cancer. *Nat Med* 2015; **21**: 1253–1261
19. Godinho M, Meijer D, Setyono-Han B et al. Characterization of BCAR4, a novel oncogene causing endocrine resistance in human breast cancer cells. *J Cell Physiol* 2011; **226**: 1741–1749
20. Gupta RA, Shah N, Wang KC et al. Long non-coding RNA HOTAIR reprograms chromatin state to promote cancer metastasis. *Nature* 2010; **464**: 1071–1076